

Electronic Supplementary Information

for

Sulfonic-acid-based lyotropic bicontinuous cubic polymer network for molecular-size-selective heterogeneous catalysis

Keira E. Culley,^a Christopher Johnson^b and Douglas L. Gin*^a

^aDepartment of Chemistry, UCB 215, University of Colorado, Boulder, CO 80309, USA

^b Department of Chemical and Biomolecular Engineering, University of Pennsylvania,
Philadelphia, PA 19104, USA

Table of Contents

- I. Materials and General Procedures
- II. Instrumentation
- III. Monomer Syntheses & Characterizations
- IV. Preparation and Physical Characterization of LLC Polymer Resins
- V. Calculation of Molecular Diameters of the BA Derivatives Tested
- VI. Setup and Monitoring of Homogeneous and Heterogeneous Acid-catalyzed Esterification Reactions
- VII. References for the ESI

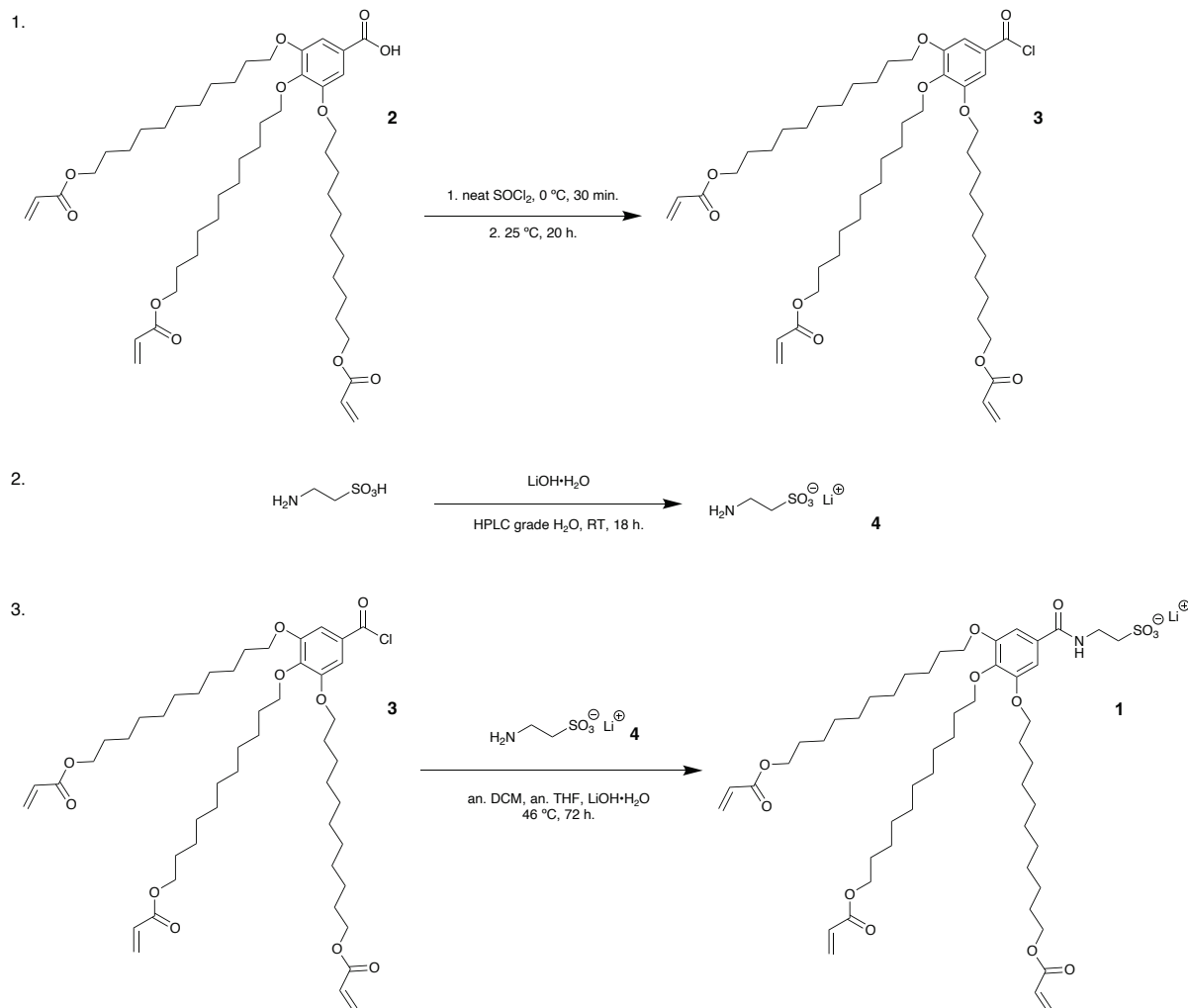
I. Materials and General Procedures

Methyl gallate, 2-hydroxy-2-methylpropiophenone (HMP (a radical photo-initiator), 97%), propylene carbonate (PC, 99.7%, anhydrous), and lithium hydroxide monohydrate (99.995%) were purchased from Sigma-Aldrich. 11-Bromoundecan-1-ol, and 2-aminoethansulfonic acid were purchased from TCI America. Normal-phase 200-400 mesh silica gel was purchased from Sorbent Technologies. Potassium hydroxide, potassium carbonate, sodium chloride, magnesium sulfate, sodium sulfate, Celite™ 545, and hydrochloric acid (all ACS reagents) were purchased from Fisher Scientific and used as received. Acryloyl chloride, purchased from Sigma-Aldrich, was freshly distilled under Ar prior to use. Dowex® 50 WX4-100 ion-exchange resin was purchased from Sigma-Aldrich and acidified before use with 12.1 M aq. hydrochloric acid. 1,4-Dioxane, purchased from Sigma-Aldrich, was distilled from a mixture with sodium benzophenone ketyl before use. Dichloromethane, tetrahydrofuran, *N,N*-dimethylformamide, *N,N*-dimethylamine (98%), and thionyl chloride were purchased from Sigma-Aldrich as anhydrous and stored in a Straus flask under Ar to maintain an air- and water-free environment. All other chemicals and solvents were purchased from either Sigma-Aldrich, TCI America, or Fisher Scientific and used without further purification. All manipulations, except for reaction work-up procedures, were performed under Ar flush using conventional Schlenk line techniques. Unless otherwise specified, organic extracts were dried over anhydrous sodium sulfate. Solvents were removed using a rotary evaporator, followed by drying on a Schlenk line ($\leq 10^{-4}$ torr).

II. Instrumentation

^1H NMR and ^{13}C NMR spectra were obtained using a Bruker AMX-300 (300 MHz for ^1H) spectrometer. Chemical shifts are reported in ppm relative to residual nondeuterated solvent. Fourier-transform infrared (FT-IR) spectroscopy measurements were performed using an Agilent Cary 630 FTIR instrument single-reflection horizontal ATR accessory with a diamond crystal. Polarized light microscopy (PLM) studies were performed with a Leica DMRXP polarizing light microscope equipped with a Q-Imaging MicroPublisher 3.3 RTV digital camera, a Linkam LTS 350 thermal stage, and a Linkam CI 94 temperature controller. An IEC Centra-CL2 centrifuge was used to isolate recycled catalyst resin powder. Powder X-ray diffraction (PXRD) spectra were obtained with an Inel CPS 120 diffraction system using monochromated Cu K_α radiation. PXRD measurements on samples were all performed at room temperature ((21 ± 1) °C). Small-angle X-ray scattering (SAXS) spectra were obtained by collaborators at the University of Pennsylvania using a Xenocs Xeuss 2.0 system in the Dual Source and Environmental X-ray Scattering (DEXS) facility at the University of Pennsylvania. A GeniX3D Cu source with a wavelength of 1.54 Å was used, with a typical sample-to-detector distance, and film samples were packed between Kapton windows. Foxtrot software was used for azimuthal integration of scattering patterns into 1-D plots of scattering intensity (I) vs. q , where $q = 4\pi\sin(\theta)/\lambda$ and the scattering angle is 2θ . Elemental analysis was performed by Galbraith Laboratories, Knoxville, TN. An LR Technologies Xtreme 206-11K Hot/Cold Plate was used to heat films during film fabrication. A BlakRay XX40BLB 40-watt (365-nm) UV lamp was used to cross-link thick, free-standing films of monomer **1** + PC + HMP. Polymer resins were powdered for catalysis experiments using a mortar and pestle and liquid nitrogen (when required). The wire-mesh sieves used for particle size separation were 3 inches in diameter, made of stainless steel, and purchased from Cole-Parmer.

III. Monomer Syntheses & Characterizations



Scheme S1. Synthesis of monomer **1**.

3,4,5-Tris(11'-acryloyloxyundecyloxy)benzoic acid (2). The carboxylic acid starting material was prepared from methyl gallate, 11-bromoundecanol, and acryloyl chloride as described in the literature.¹ Characterization data agreed with those reported in the literature.¹

3,4,5-Tris(11'-acryloyloxyundecyloxy)benzoyl chloride (3): This compound was prepared from compound **2** and thionyl chloride as described in the literature,² with the following modifications: compound **2** was dissolved in neat thionyl chloride (20x excess, or enough to dissolve all of the solids) at 0 °C in an ice bath. The solution was stirred at 0 °C for 30 min, and then allowed to gradually warm to room temperature (RT) (ca. 21 °C) and stirred overnight. The thionyl chloride was removed under reduced pressure using a Schlenk line and a glass vapor condensation trap cooled with liquid nitrogen (see Fig. S1). The product was used immediately and without any further purification due to the high reactivity. The product was never exposed to air or water.²

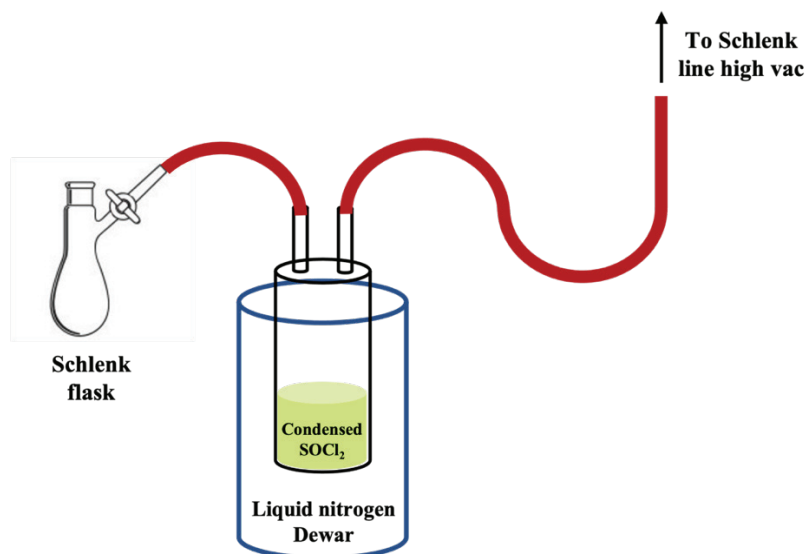
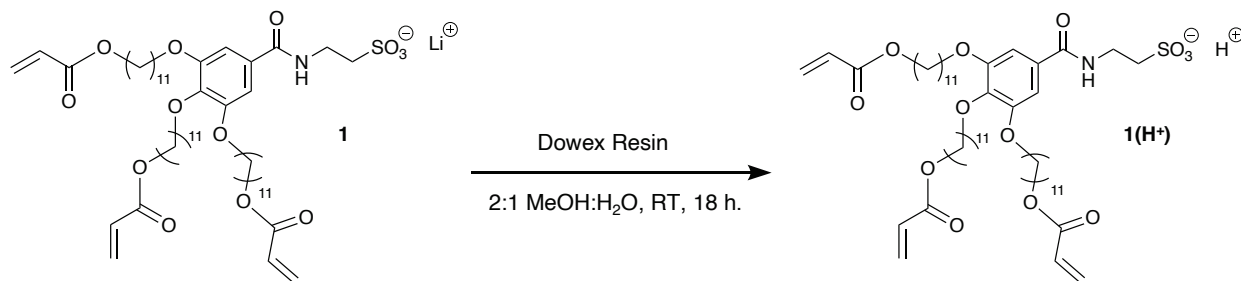


Fig. S1 Schematic of the apparatus used to safely remove excess SOCl₂ from the reaction flask without damaging any vacuum equipment (rotary evaporator or Schlenk line).

Lithium-2-aminoethanesulfonate (4): This compound was prepared from 2-aminoethanesulfonic acid and lithium hydroxide monohydrate as described in the literature,² with the following modifications: HPLC grade water was used instead of Pestanal® water. Characterization data agreed with those reported in the literature.²

Lithium-2-(3,4,5-tris(11'-acryloyloxy)undecyloxy)benzamido)-ethanesulfonate (1): This compound was prepared from compound 3, compound 4, and lithium hydroxide monohydrate as described in the literature,² with the following modifications: 75 mL of dry CH₂Cl₂ was used to dissolve compound 3 instead of 125 mL, and a cold finger condenser was used to prevent evaporation of the CH₂Cl₂ during the 72-h reflux period. Characterization data agreed with those reported in the literature.²



Scheme S2. Synthesis of monomer **1(H⁺)**.

2-(3,4,5-Tris(11'-acryloyloxy)undecyloxy)benzamido)-ethanesulfonic acid (1(H⁺)): Monomer **1** (0.5648g, 0.591 mmol) was dissolved in a 2:1 (v/v) MeOH : deionized (DI) H₂O solution in a

round-bottom flask with a magnetic stir bar. Freshly acidified Dowex® resin (excess) was added to the flask, and the mixture was stirred overnight at RT. The Dowex® resin was then removed using a Buchner funnel, and the MeOH : DI H₂O solution was filtered through a silica plug to remove any Li⁺ salt impurities. Evaporation of the solvent under reduced pressure gave monomer **1(H⁺)** as a light yellow semi-solid. (0.5456g, 0.574 mmol, 97% yield). ¹H NMR (300 MHz, DMSO-*d*₆) δ 8.44 (t, *J* = 5.4 Hz, 1H), 7.07 (s, 2H), 6.61 – 5.81 (m, 6H), 4.76 (s, 5H), 4.06 (dt, *J* = 10.9, 6.5 Hz, 6H), 3.97 (t, *J* = 6.1 Hz, 4H), 3.87 (t, *J* = 6.3 Hz, 2H), 3.79 (t, *J* = 6.2 Hz, 2H), 3.50 (t, *J* = 6.7 Hz, 2H), 2.80 (t, *J* = 6.2 Hz, 2H), 2.67 (dd, *J* = 8.1, 6.3 Hz, 2H), 1.72 (t, *J* = 7.2 Hz, 4H), 1.60 (h, *J* = 6.3 Hz, 8H), 1.42 (d, *J* = 6.9 Hz, 8H), 1.27 (s, 37H). ¹³C NMR (75 MHz, DMSO-*d*₆): 166.12, 166.10, 165.86, 152.86, 140.09, 131.92, 130.13, 129.03, 129.02, 105.95, 73.03, 68.97, 64.70, 64.68, 51.11, 40.78, 40.58, 40.37, 40.16, 39.95, 39.74, 39.53, 36.87, 30.48, 29.84, 29.75, 29.72, 29.66, 29.61, 29.52, 29.48, 29.39, 29.37, 28.77, 26.32, 26.09, 26.07. FT-IR (neat): 3321, 3101, 2922, 2851, 1725, 1636, 1580, 1546, 1498, 1468, 1427, 1334, 1189, 1110, 1047, 984, 861, 809, 723, 670. Elemental Analysis: Calcd for C₅₀H₈₃NO₁₃S: C, 64.01; H, 8.92; N, 1.49; Li, 0.00. Calcd for C₅₀H₈₃NO₁₃S•3H₂O: C 60.99; H, 8.93; N 1.39; Li, 0.00. Found: C, 60.79; H, 8.69; N, 1.39; Li, 0.0121. Elemental analysis for C, H, and N content was performed by combustion analysis, and elemental analysis for Li content was performed by inductively coupled plasma (ICP) spectroscopy.

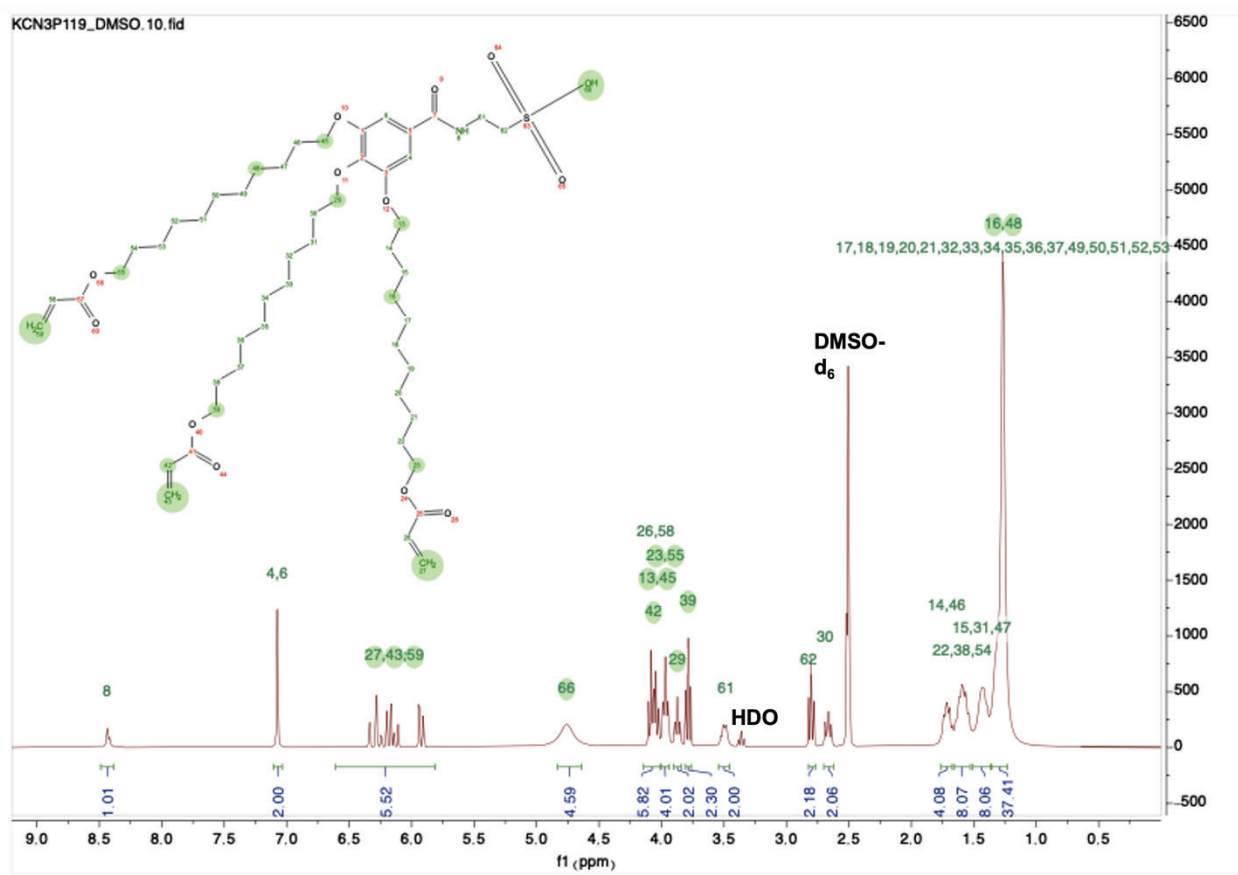


Fig. S2 ¹H NMR spectrum of monomer **1(H⁺)** in DMSO-*d*₆ (the peaks at 2.50 ppm and 3.33 ppm are from residual DMSO in the deuterated solvent). ¹H NMR assignments were confirmed through ¹H-¹H 2D-NMR correlation spectroscopy (COSY).

IV. Preparation and Physical Characterization of LLC Polymer Resins

General procedure for preparation and characterization of a (Q_{II} resin of 1)/Li⁺ bulk film³

This material was prepared similar to that reported in the literature,³ but using the following slightly modified procedure: Monomer **1** (84 wt%), PC (15 wt%), and HMP (1 wt%) were added to a 1-dram glass vial and mixed by hand with a spatula until the mixture appeared homogeneous by eye (5–10 min). The mixture was sandwiched between two Mylar® sheets, annealed at 70 °C on a hot plate for ca. 2 min, cooled to RT for ca. 5 min, and photopolymerised at 365 nm under a UV lamp for 1 h at RT with a light intensity (I) of >1 mW/cm² at the sample surface.

The formation of the Q_{II} phase by the monomer upon addition of PC and its retention after photopolymerisation was confirmed by its optically black appearance under PLM and by SAXS analysis (see Figs. S3 and S4). Specifically, assignment of a Q phase was done by confirming the presence of a black, pseudo-isotropic optical texture (a consequence of the cubic symmetry when subjected to polarized light) and periodic order as seen by X-ray diffraction analysis.⁴ Q phases typically exhibit PXRD peaks with a *d*-spacing pattern of $1/\sqrt{6} : 1/\sqrt{8} : 1/\sqrt{14} : 1/\sqrt{16} : 1/\sqrt{18} : 1/\sqrt{20}$ for double gyroid ($Ia\bar{3}d$) or $1/\sqrt{2} : 1/\sqrt{3} : 1/\sqrt{4} : 1/\sqrt{6} : 1/\sqrt{8} : 1/\sqrt{9}$ for $Pn\bar{3}m$ with respect to the principal peak, corresponding to SAXS peaks at particular ratios of scattering vectors (*e.g.*, $\sqrt{6} : \sqrt{8} : \sqrt{14} : \sqrt{16} : \sqrt{18} : \sqrt{20}$ for double gyroid ($Ia\bar{3}d$) or $\sqrt{2} : \sqrt{3} : \sqrt{4} : \sqrt{6} : \sqrt{8} : \sqrt{9}$ for $Pn\bar{3}m$).^{4–6} Q phases are optically transparent but are typically very viscous in nature because they consist of 3D-interpenetrating hydrophobic and hydrophilic channels.^{4–6}

In contrast, H phases have PXRD peaks with a *d*-spacing pattern of $1 : 1/\sqrt{3} : 1/\sqrt{4} : 1/\sqrt{7} : 1/\sqrt{9} \dots$ etc. with respect to the principal peak, corresponding to SAXS peaks at scattering vectors with the ratios $1 : \sqrt{3} : \sqrt{4} : \sqrt{7} : \sqrt{9} \dots$ etc.^{4,6} L phases have PXRD peaks with a *d*-spacing pattern of $1 : 1/2 : 1/3 : 1/4 : 1/5 \dots$ etc. with respect to the principal peak, corresponding to SAXS peaks at scattering vectors with the ratios $1 : 2 : 3 : 4 : 5 \dots$ etc.^{4,6}

In addition, each LLC phase with the specific geometry/symmetry described above can also be sub-classified in terms of whether the hydrophilic–hydrophobic interface curves away from (*i.e.*, type I, normal) or toward the aqueous / polar solvent regions (*i.e.*, type II, reverse).^{4,6} To unequivocally determine whether an observed LLC phase is type I or type II, an L phase needs to be present in the phase diagram as a central reference point that has no preferred net curvature towards either the hydrophilic or hydrophobic domains.^{4,6} Then, LLC phases on the water- or polar solvent-excessive side of the L phase can be assigned as type I (*i.e.*, normal) phases, and those on the water- or polar solvent-deficient side can be assigned as type II (*i.e.*, reverse) phases.⁶ As detailed in a prior paper, the presence of an observed L phase at higher PC content for monomer **1** indicates that it forms a Q_{II} phase with PC.²

Note: PXRD and SAXS studies were not able to resolve enough diffraction peaks in the Q_{II}-phase samples of monomer **1** + PC or the resulting Q_{II}-phase resins to unequivocally identify the type of unit cell. However, $Ia\bar{3}d$ and $Pn\bar{3}m$ space groups are frequently observed for Q LLC phases reported in literature, and we speculate that the system here corresponds to one of those.⁶

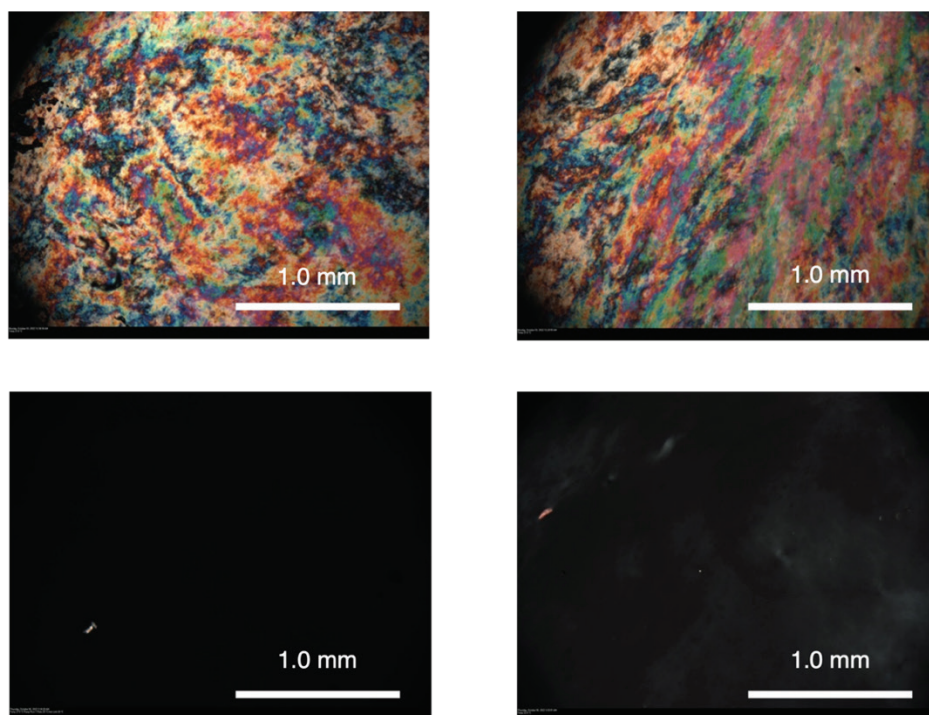


Fig. S3 PLM images of a) a mixture of 84 wt% **1**, 15 wt% PC, and 1 wt% HMP) at 25 °C prior to photopolymerisation without an annealing step; b) a mixture of 84 wt% **1**, 15 wt% PC, and 1 wt% HMP at 25 °C prior to photopolymerisation without an annealing step; c) a mixture of 84 wt% **1**, 15 wt% PC, and 1 wt% HMP at 25 °C prior to photopolymerisation with an annealing step; and d) a bulk film of the (Q_{II} resin of **1**)/ Li^+ at 25 °C that was formed by photo-cross-linking a mixture of 84 wt% **1**, 15 wt% PC, and 1 wt% HMP at RT with an annealing step.

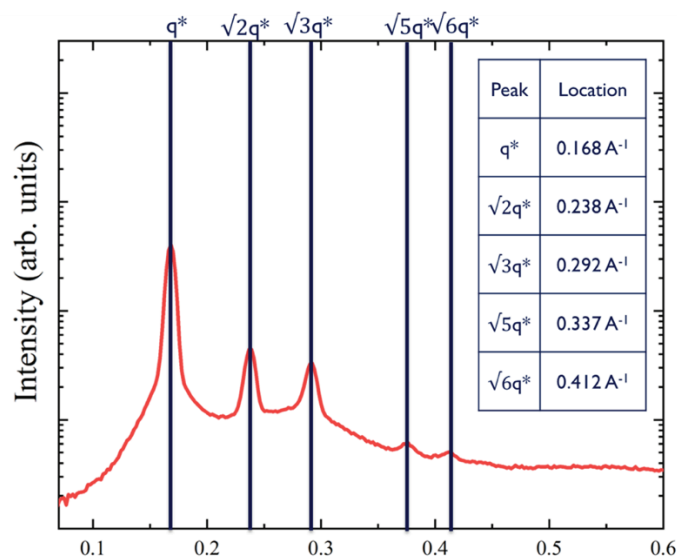


Fig. S4 Characteristic SAXS spectrum of a Q_{II} monomer mixture of 84 wt% **1**, 15 wt% PC, and 1 wt% HMP at RT prior to photopolymerisation.

The degree of acrylate polymerisation was determined by comparing the intensity of the acrylate C=C band at 812 cm^{-1} before and after photopolymerisation using FT-IR spectroscopy, as previously reported in the literature.² The complete disappearance of the 812 cm^{-1} band after photopolymerisation indicated essentially complete acrylate polymerisation (see Fig. S5).

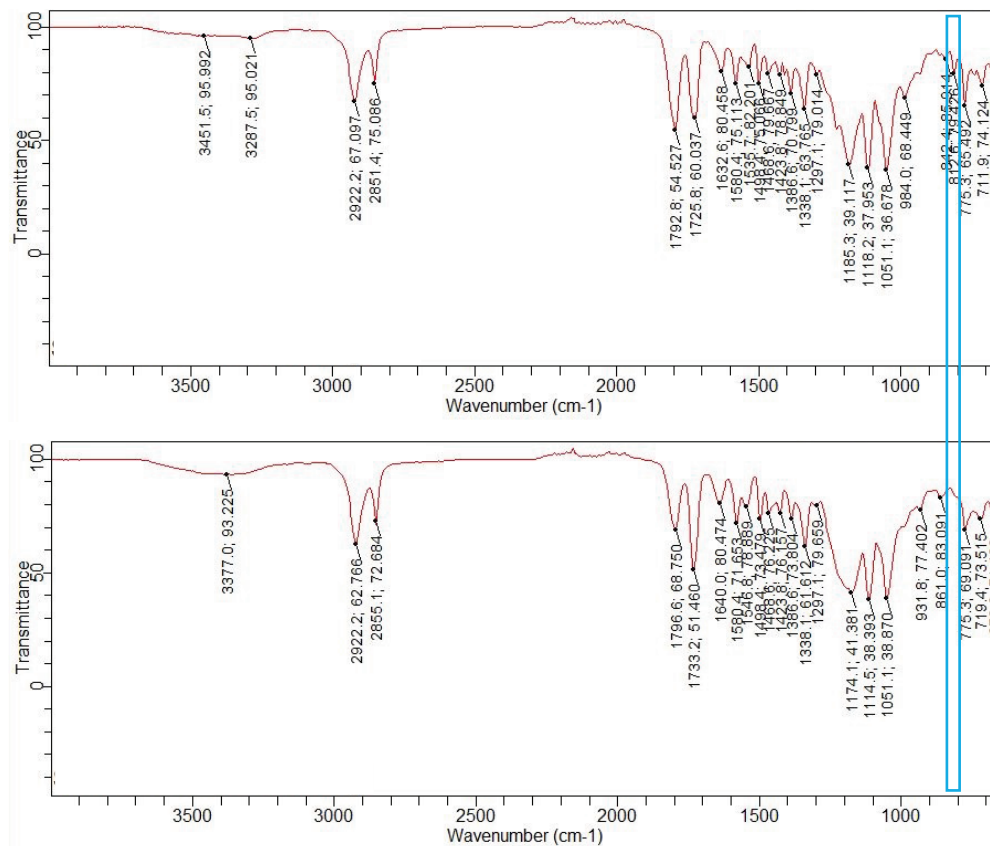


Fig. S5 FT-IR spectra of a mixture of 84 wt% **1**, 15 wt% PC, and 1 wt.% HMP before (top spectrum) and after photopolymerisation (bottom spectrum) at RT. The disappearance of the characteristic acrylate peak at 812 cm^{-1} (region boxed in blue) indicates complete polymerisation.

General procedure for preparation of the (Q_{II} resin of **1**)/ H^+ from the (Q_{II} resin of **1**)/ Li^+

A bulk film sample of the (Q_{II} resin of **1**)/ Li^+ was placed in a 1-dram glass vial or centrifuge tube, and the vial was filled with 1 M aq. HCl. The vial was agitated to make sure the entire bulk film was submerged in the acid solution, and was allowed to soak overnight to initiate the cation exchange to give a bulk film of (Q_{II} resin of **1**)/ H^+ . After soaking for 24 h, the aqueous acid solution was then removed from the vial by syringe and replaced with DI H_2O to soak for another 24 h. After soaking for 24 h in DI H_2O , the water was removed, and fresh DI H_2O was added. This process was continued until the water layer was a pH of 7. The bulk film of (Q_{II} resin of **1**)/ H^+ was then removed and dried in air at RT.

Retention of the Q_{II} phase in the resulting acidified (**Q_{II} resin of 1**)/ H^+ bulk film was confirmed by PLM and SAXS analysis, as described above for the initial Q_{II} -phase Li-salt film (see Fig. S6 for example SAXS spectra).

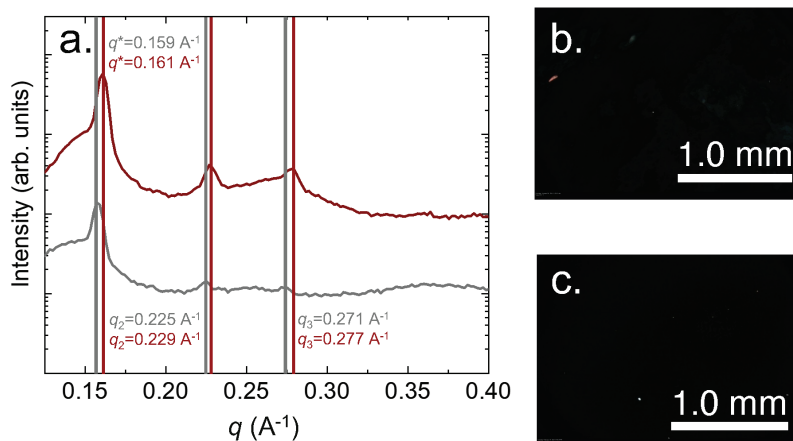


Fig. S6 (a) SAXS spectra of the (**Q_{II} resin of 1**)/ Li^+ (red line) and of the (**Q_{II} resin of 1**)/ H^+ (grey line) sample produced after H^+ for Li^+ exchange. PLM images of the materials (mag = 50x): (b) before acidification and (c) after acidification.

The amount of residual Li in the (**Q_{II} resin of 1**)/ H^+ film after acidification was determined by elemental analysis to be 0.0121%.

The resulting bulk film of (**Q_{II} resin of 1**)/ H^+ was then powdered using a mortar and pestle and sieved to a 75–150 μm particle size using wire-mesh sieves.³ Note: The bulk films of the (**Q_{II} resin of 1**)/ H^+ should be pliable but should snap upon bending in half and crush easily into a fine white powder. Retention of the Q_{II} phase in the powdered resins was confirmed by SAXS analysis as shown in Fig. S7 below.

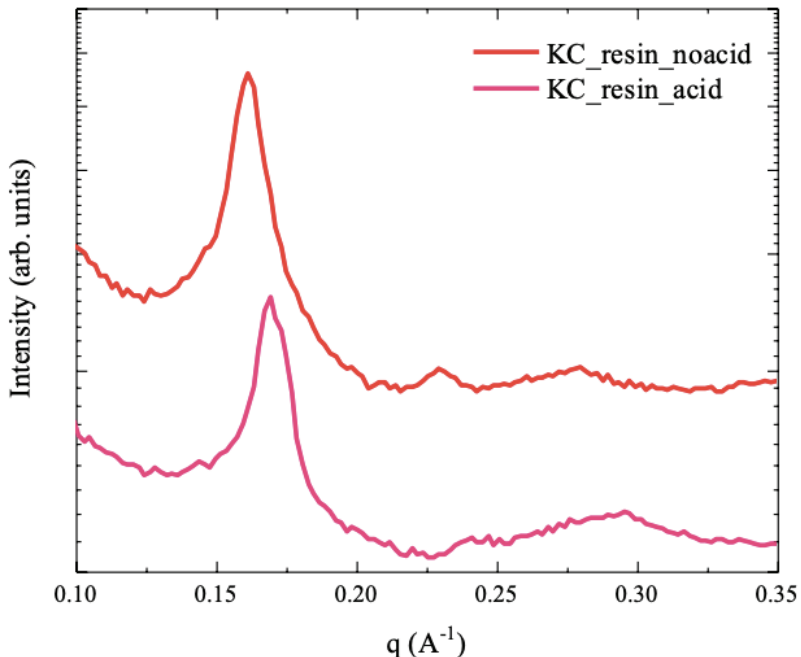


Fig. S7 SAXS spectra of the (**Q_{II} resin of 1**)/Li⁺ in powder form (top trace, red) and of the (**Q_{II} resin of 1**)/H⁺ in powder form (bottom trace, magenta), showing Q_{II} phase retention after acidification and grinding into particles.

Prior Unsuccessful Attempts to Use BET Gas Adsorption Analysis to Characterize LLC Network Nanopores and Surface Area

The Gin group has previously attempted pore characterization and surface area measurements on LLC polymer networks using standard BET gas adsorption techniques and found that these methods are not effective at providing an accurate estimate of the pore area or pore structure in these materials^{7,8} (see the data and discussions in the Supporting Information for References 7 and 8). This is because it is not possible to completely remove the solvent molecules (e.g., water) in LLC network nanopores: There are very high capillary forces in the nanopores, and the ionic headgroups in these pores coordinate with solvent molecules and remain partially solvated even after rigorous drying under vacuum at elevated temperatures and lyophilization attempts. The residual solvent molecules restrict the entry of gas molecules into the pores and occupy pore volume that would otherwise adsorb gas molecules, leading to observed significant underestimations of the actual pore area.^{7,8} In addition, other researchers who recently used BET gas adsorption analysis to try and characterize the pore sizes and surface areas of LLC polymer membranes have seen similar inconsistencies and large variations in their results.⁹

Preparation of (mixed-phase resin of 1)/H⁺ for substrate size-selectivity control experiments

Attempts were made to make a different-phase solid resin catalyst with the exact same chemical composition as (**Q_{II} resin of 1**)/H⁺ (84 wt% **1**, 15 wt% PC, and 1 wt% HMP mixture followed by polymerisation and ion exchange to the acid form), however this composition was found to retain the Q_{II} phase by PLM and PXRD from RT to 150 °C. Therefore, the composition of the resin had

to be adjusted to obtain a mixed-phase or a different-phase control resin. The procedure to obtain the **(mixed-phase resin of 1)/H⁺** was as follows:

Monomer **1** (99 wt%) and HMP (1 wt%) were added to a 1-dram glass vial and mixed by hand with a spatula at RT until the mixture appeared homogeneous by eye (5–10 min). The mixture was sandwiched between two Mylar® sheets and photopolymerised at 365 nm under a UV lamp for 1 h at RT. The lack of cohesive nanostructure in this sample was verified by the appearance of a mixed, bright optical texture under PLM (indicating some anisotropic (*i.e.*, non-Q-phase) LC order) and PXRD peaks that do not match a pure Q phase (see Fig. S8).

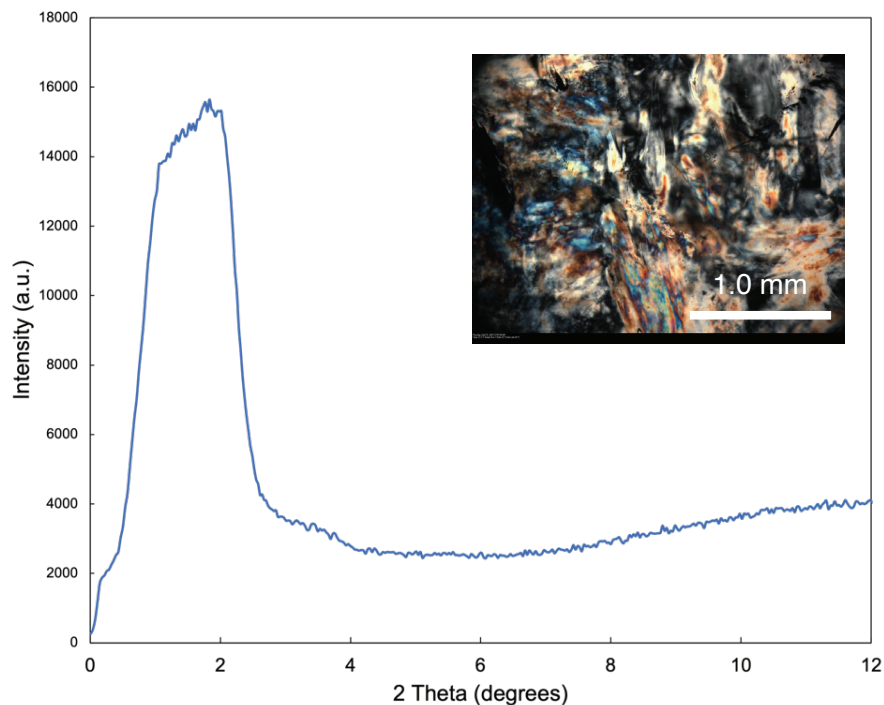


Fig. S8 PXRD profile and PLM optical texture of the solid-state **(mixed-phase resin of 1)/H⁺** control catalyst.

V. Calculation of Molecular Diameters of the BA Derivatives Tested

To determine the approximate molecular diameters of the BA derivatives tested, their structures were drawn using MarvinSketch and then geometry-optimized in 3D based on parameters from the Dreiding forcefield using the “Clean in 3D” function built into MarvinSketch.³ Using the optimized structure and geometrical descriptors tool, we were able to deduce the projection radius (in Å) for DM-BA and DP-BA. The calculated molecular diameters of BA and BT-BA were previously reported in the literature using the same method.³

Table S1 Compilation of calculated molecular diameters for the four tested BA derivatives using MarvinSketch.

Alcohol	Longest Molecular Diameter (Å)
benzyl alcohol (BA)	6.9
3,5-dimethoxybenzyl alcohol (DM-BA)	9.8
3,5-bis(benzyloxy)benzyl alcohol (DP-BA)	12.5
3,5-bis(<i>tert</i> -butyldiphenylsilyloxy)benzyl alcohol (BT-BA)	16.8

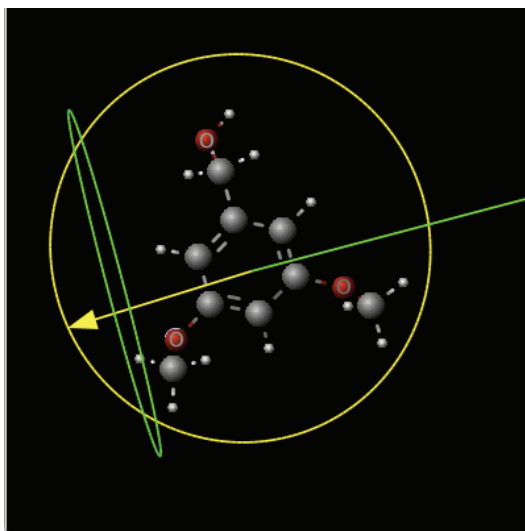


Fig. S9 Example image of the geometrical descriptors tool in MarvinSketch that were used to estimate the maximum molecular diameter of DM-BA.

VI. Setup and Monitoring of Homogeneous and Heterogeneous Acid-catalyzed Esterification Reactions

General procedure for the esterification control reactions with no added catalyst

An equimolar amount of 1-hexanoic acid and BA derivative (0.25 M) were added to a flame-dried Schlenk flask with the appropriate amount of anhydrous toluene to keep the molarity of the reactants at 0.25 M. The reaction was heated to 75 °C using an oil bath and stirred under a static atmosphere of Ar for 20 h. After 20 h, the reaction was cooled to RT, the toluene was removed under reduced pressure, and the residue was analyzed by ¹H NMR spectroscopy to assess percent conversion of alcohol to ester.

General procedure for the homogeneous (*i.e.*, solution-state) esterification reactions catalyzed by monomer **1(H⁺)**

Equimolar amounts of 1-hexanoic acid (1 equiv.) and BA or BA derivative (1 equiv.) were added to a flame-dried Schlenk flask with the appropriate amount of anhydrous toluene to keep the molarity of the reactants at 0.25 M. Monomer **1**(H⁺) (0.05 equiv. based on SO₃H sites) was dissolved in a portion of the toluene and added to the reaction by syringe. The reaction was heated to 75 °C in an oil bath and stirred under static Ar for 20 h. After 20 h, the reaction was cooled to RT, the toluene was removed under reduced pressure, and the residue was analyzed by ¹H NMR spectroscopy to assess percent conversion of alcohol to ester.

General procedure for the heterogeneous esterification reactions catalysed by powdered (Q_{II} resin of 1**)/H⁺**

Equimolar amounts of 1-hexanoic acid (1 equiv.) and BA or BA derivative (1 equiv.) were added to a flame-dried Schlenk flask with the appropriate amount of anhydrous toluene to keep the molarity of the reactants at 0.25 M. The powdered (**Q_{II} resin of 1**)/H⁺ (0.05 equiv. based on SO₃H sites in the resin composition) was added to the reaction under Ar flush. The reaction was heated to 75 °C in an oil bath and stirred under static Ar for 163 h with aliquots of the reaction taken at 2, 4, 6, 20, 24, 48, 72, and 163 h. Conversion of the BA or BA derivative to the corresponding ester was assessed by ¹H NMR spectroscopy (see Figs. S10–S12 for example data).

Determination of esterification percent conversion by ¹H NMR analysis

Calculation: Percent conversion was calculated using the integration values for the characteristic CH₂OH and CH₂(O)R signals of the BA derivatives and the expected ester products with 1-hexanoic acid, respectively. Example product-mixture ¹H NMR spectra and percent conversion calculations are shown in Figs. S10–S12 for the reaction of different BA derivatives with 1-hexanoic acid using the various acid catalysts tested (20 h reaction time).

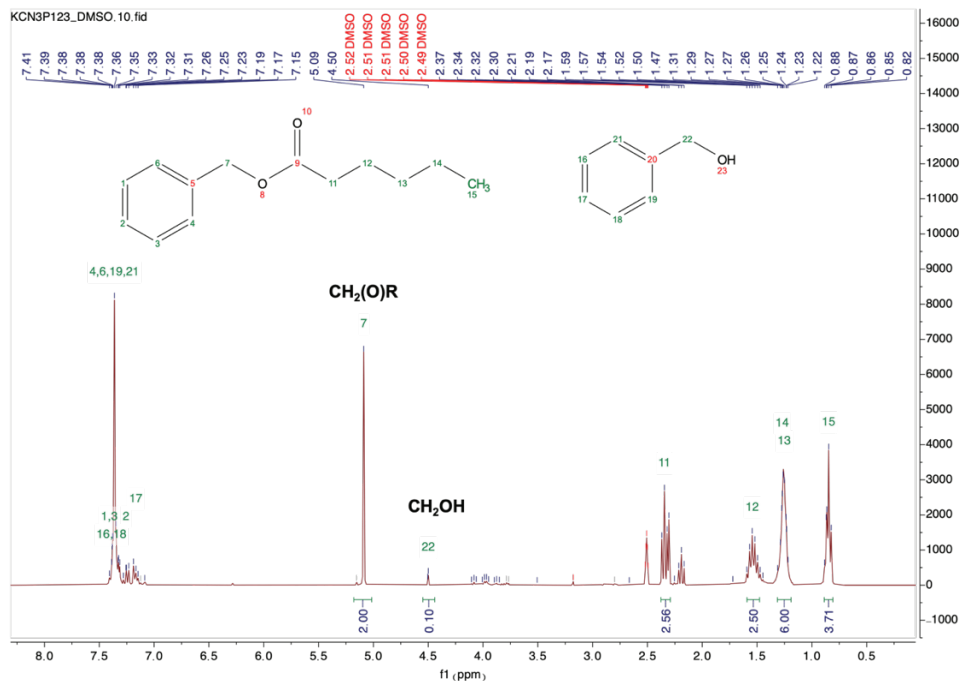


Fig. S10 Example ^1H NMR spectrum monitoring the conversion of BA upon reaction with 1-hexanoic acid to the ester product using monomer **1**(H^+) as a solution-state acid catalyst, with peak assignments and integration values. NMR spectrum taken in $\text{DMSO-}d_6$ (the peaks at 2.50 and 3.33 ppm are from residual DMSO in the deuterated solvent).

$$\text{Percent conversion} = \frac{\text{ester } \text{CH}_2(\text{O})\text{R integral}}{\text{ester integral} + \text{BA } \text{CH}_2\text{OH integral}} \times 100$$

$$\text{Percent conversion} = \frac{2.00}{2.00 + 0.10} \times 100 = 95\%$$

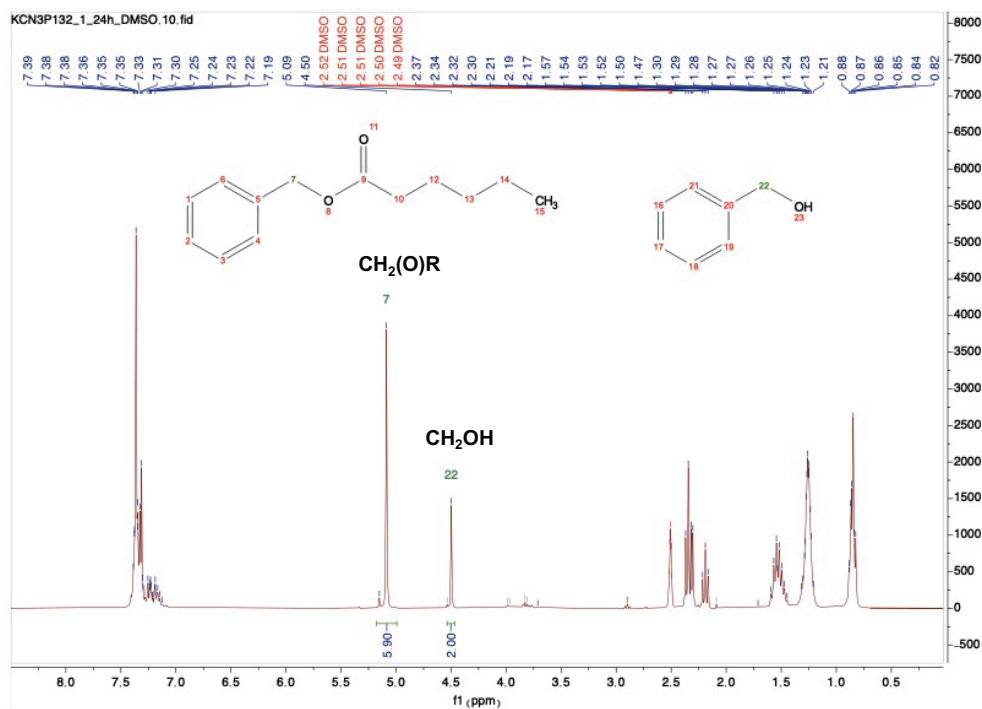


Fig. S11 Example ^1H NMR spectrum monitoring the conversion of BA upon reaction with 1-hexanoic acid to the ester product using (**Q_{II} resin of 1**)/ H^+ as a solid-state acid catalyst, with peak assignments and integration values. NMR spectrum taken in $\text{DMSO-}d_6$ (the peaks at 2.50 and 3.33 ppm are from residual DMSO in the deuterated solvent).

$$\text{Percent conversion} = \frac{\text{ester } \text{CH}_2(\text{O})\text{R integral}}{\text{ester integral} + \text{BA } \text{CH}_2\text{OH integral}} \times 100$$

$$\text{Percent conversion} = \frac{5.90}{5.90 + 2.00} \times 100 = 75\%$$

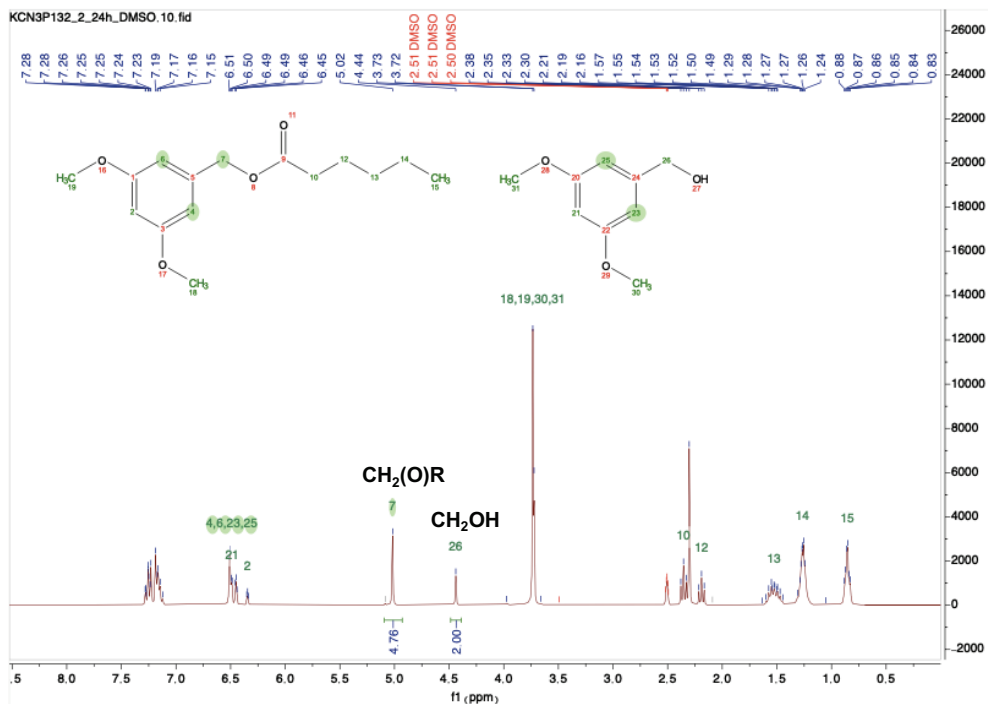


Fig. S12 Example ¹H NMR spectrum monitoring the conversion of DM-BA upon reaction with 1-hexanoic acid to the ester product using (**Q_{II} resin of 1**)/H⁺ as a solid-state acid catalyst, with peak assignments and integration values. NMR spectrum taken in DMSO-*d*₆ (the peaks at 2.50 and 3.33 ppm are from residual DMSO in the deuterated solvent), and residual anhydrous toluene is seen at 2.3 ppm and 7.12–7.35 ppm.

$$\text{Percent conversion} = \frac{\text{ester } CH_2(O)R \text{ integral}}{\text{ester integral} + \text{DM-BA } CH_2OH \text{ integral}} \times 100$$

$$\text{Percent conversion} = \frac{4.76}{4.76 + 2.00} \times 100 = 70\%$$

Table S2 Summary of solution-state catalytic activity of monomer **1(H⁺)** for the reaction of increasingly sized BA derivatives with 1-hexanoic acid. Reaction conditions: 5 mol% SO₃H sites relative to the BA derivative and 1-hexanoic acid substrates, anhydrous toluene solvent, 75 °C, 20 h reaction time. Values shown are average values over 3 independent runs with standard deviation error bars.

Entry	Alcohol	Catalyst	Reaction Conversion in 20 h (%)
A	BA	None	Not detected
B	BA	1(H⁺) (soln)	87 ± 7
C	DM-BA	None	Not detected
D	DM-BA	1(H⁺) (soln)	80 ± 1
E	DP-BA	None	Not detected
F	DP-BA	1(H⁺) (soln)	85 ± 5
G	BT-BA	None	Not detected
H	BT-BA	1(H⁺) (soln)	38 ± 5

Table S3 Comparison of substrate conversion and alcohol reagent molar selectivity (DM-BA/BT-BA and DP-BA/BT-BA) in the presence of solution-state monomer acid catalyst **1(H⁺)** and solid-state acid catalyst (**Q_{II} resin of 1**)/H⁺. Reaction conditions: 5 mol% SO₃H sites relative to alcohol and carboxylic acid substrates, anhydrous toluene solvent, 75 °C, 20 h reaction time. Values shown are average values over 3 independent runs with standard deviation error bars.

Entry	Catalyst	DM-BA conversion in 20 h (%)	DP-BA conversion in 20 h (%)	BT-BA conversion in 20 h (%)	Molar selectivity (DM-BA/BT-BA)	Molar selectivity (DP-BA/BT-BA)
A	None	Not detected	Not detected	Not detected	n/a	n/a
B	1(H⁺) (soln)	80 ± 1	85 ± 5	38 ± 5	2.1 ± 0.2	2.3 ± 0.3
C	(Q_{II} resin of 1)/H ⁺	58 ± 5	60 ± 2	2 ± 1	25 ± 5	26 ± 5

General procedure for (**Q_{II} resin of 1**)/H⁺ heterogeneous catalyst resin recycling and reuse studies

Equimolar amounts of 1-hexanoic acid (1 equiv.) and BA or BA derivative (1 equiv.) were added to an oven-dried 3-dram glass vial with the appropriate amount of anhydrous toluene to keep the molarity of the reactants at 0.25 M. The appropriate amount of powdered and sieved (**Q_{II} resin of 1**)/H⁺ (0.05 equiv. SO₃H groups relative to the reactants based on resin composition) was added to the reaction. The reaction was heated to 75 °C in an oil bath under Ar flush, capped, and stirred for 20 h. The vial was centrifuged, and the solution was removed by syringe and concentrated. Conversion of BA to ester was determined by ¹H NMR spectroscopy, as described in the prior section.

The recovered (**Q_{II} resin of 1**)/H⁺ from the previous step was soaked in hexanes in the same 3-dram vial at RT for 10 min. The vial was then centrifuged again for 5 min at 4000 rpm and the supernatant was discarded. The washing process was repeated until the hexanes wash solution came back clean by ¹H NMR analysis (approximately 5 times). This indicated that there were no remaining starting materials or product in the vial. The powdered resin was then dried in vacuo at RT using a Schlenk line, re-weighed, and 1-hexanoic acid and BA reactants were added to the vial according to the above procedure. This process was repeated three times to assess the recyclability of the catalyst (see Fig. S13).

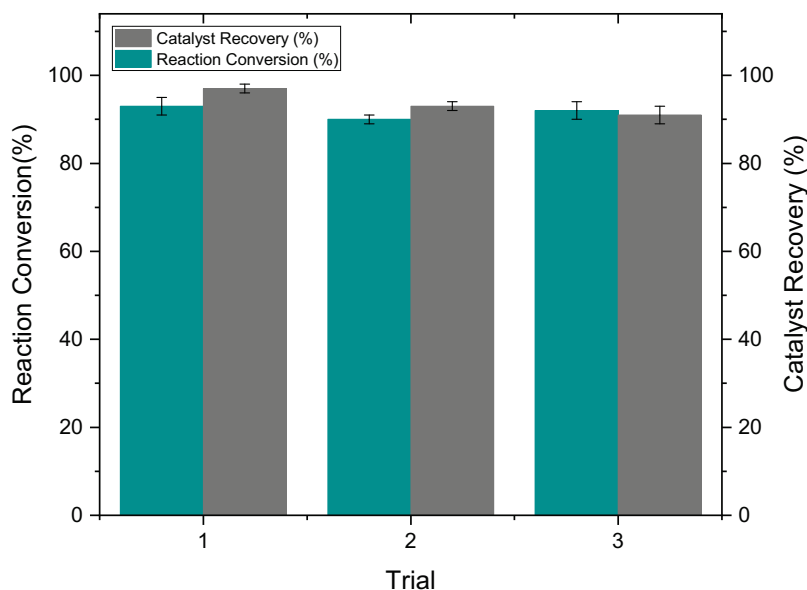
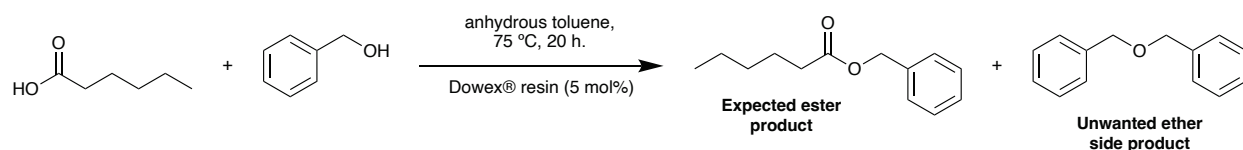


Fig. S13 Percent conversion to ester (green bars) and percent recovery of the catalyst (grey bars) after 20 h of reaction for three successive recycling experiments using the same (**Q_{II} resin of 1**)/H⁺ sample as the catalyst. Reaction conditions: 5 mol% SO₃H sites relative to alcohol and carboxylic acid substrates based on catalyst resin composition, anhydrous toluene solvent, 75 °C, 20 h reaction time. Values shown are average values over 3 independent runs with standard deviation error bars.

Preparation and use of Dowex® resin for substrate-size-selectivity control experiments and analysis of control reactions

Scheme S3 below shows the major competing reaction products that can be formed in the heterogeneous sulfonic-acid-catalyzed reaction between BA and 1-hexanoic acid in anh. toluene at 75 °C, as previously reported.¹⁰ Nanostructured (**Q_{II} resin of 1**)/H⁺ (with uniform acidic nanopores) was compared against Dowex® 50WX4-100, H⁺ form (a commercial, amorphous, polystyrenesulfonic-acid-based gel-type resin¹¹) as an acid catalyst in this reaction, in order to examine the contribution of a regular, nanoporous structure in the catalyst. Dowex® 50WX4, H⁺ form and other related cross-linked polystyrenesulfonic acid resins have been used as heterogeneous acid catalysts for organic transformations.¹¹



Scheme S3 Reaction scheme of the competing products produced in the reaction of BA with 1-hexanoic acid using commercial, amorphous Dowex® 50WX4 resin, H⁺ form resin as a heterogeneous acid catalyst, resulting in low ester/ether molar selectivity.

The Dowex® resin was re-acidified before use since the resin was not newly purchased. The resin was placed in a round-bottom flask and stirred overnight at RT in 12.1 M aq. HCl. The mixture was then filtered through a Buchner funnel with 2–3 filter papers to recover the acidified resin.

The ester/ether (mol/mol) selectivity for the Dowex®-resin-catalysed reactions was found to be 0.6 ± 0.1 due to the non-uniform-sized pores with varying acidity (see Fig. S14 for example ¹H NMR reaction product data).

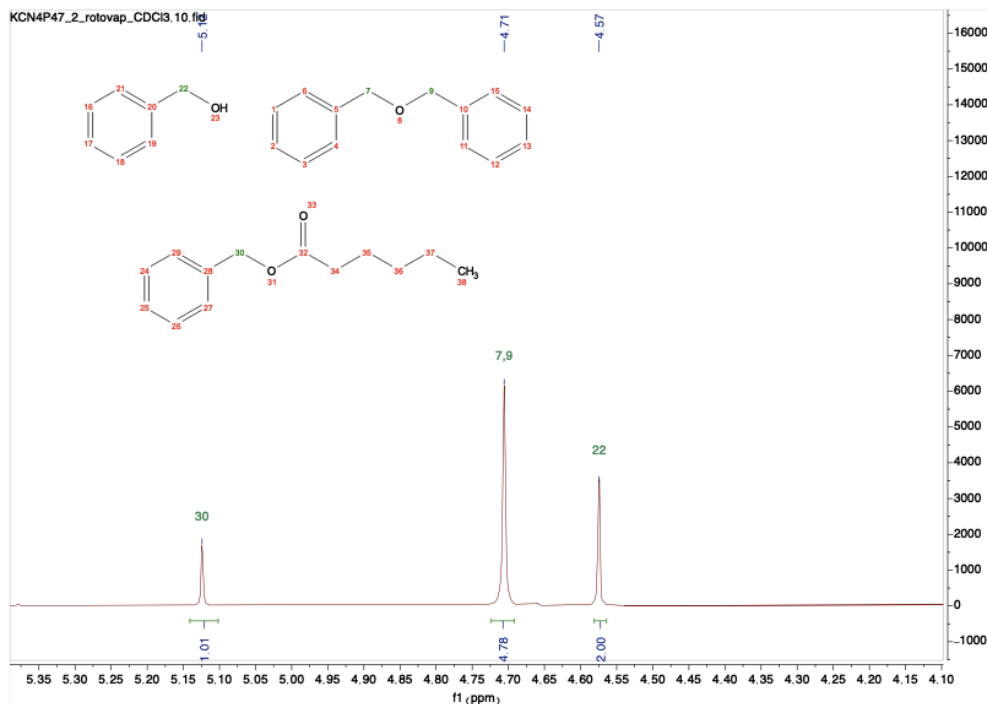


Fig. S14 Example ¹H NMR spectrum monitoring the conversion of BA to the ester product (catalysed by amorphous Dowex® 50WX4 resin, H⁺ form) and the unwanted dibenzyl ether product with relevant peak assignments and integration values.

In contrast, the (Q_{II} resin of 1)/H⁺ gave an ester/ether (mol/mol) selectivity of $(6.1 \pm 0.5) \times 10^3$ for the reaction of BA and 1-hexanoic acid – essentially only producing a single, pure organic product (see Fig. S10 for example data). This same phenomenon was seen previously in our group using an H_{II}-phase Brønsted acid catalyst in the same reaction compared to commercial, amorphous Amberlyst-15® and Nafion NR50® sulfonic-acid resins.⁷

VII. References for the ESI

- (1) O. Q. Imran, N. K. Kim, L. N. Bodkin, G. E. Dwulet, X. Feng, K. Kawabata, M. Elimelech, D. L. Gin and C. O. Osuji, *Adv. Mater. Interfaces*, 2021, **8**, 2001977.
- (2) R. L. Kerr, S. A. Miller, R. K. Shoemaker, B. J. Elliott and D. L. Gin, *J. Am. Chem. Soc.*, 2009, **131**, 15972.
- (3) G. E. Dwulet and D. L. Gin, *Chem. Commun.*, 2018, **54**, 12053.
- (4) P. Li, M. I. Reinhardt, S. S. Dyer, K. E. Moore, O. Q. Imran and D. L. Gin, *Soft Matter*, 2021, **17**, 9259.
- (5) B. R. Wiesenauer and D. L. Gin, *Polym. J.*, 2012, **44**, 461.
- (6) For general reviews on LLC phases and their classifications, see: (a) M. W. Tate, E. F. Eikenberry, D. C. Turner, E. Shyamsunder and S. M. Gruner, *Chem. Phys. Lipids*, 1991, **57**, 147. (b) J. M. Seddon, *Biochim. Biophys. Acta*, 1990, **1031**, 1. (c) G. J. T. Tiddy, *Phys. Rep.*, 1980, **57**, 1.
- (7) C. S. Pecinovsky, G. D. Nicodemus and D. L. Gin, *Chem. Mater.* 2005, **17**, 4889.
- (8) G. E. Dwulet and D. L. Gin, *Chem. Commun.* 2018, **54**, 12053.
- (9) L. Santiago-Martoral, A. Figueroa and E. Nicolau, *ACS Omega*, 2020, **5**, 17940.
- (10) Y. Xu, W. Gu and D. L. Gin, *J. Am. Chem. Soc.*, 2004, **126**, 1616.
- (11) E. Ramírez, R. Bringué, C. Fité, M. Iborra, J. Tejero and F. Cunill, *Appl. Catal. A, Gen.*, 2021, **612**, 117988.